

Resolving the atmospheric octant by an improved measurement of the reactor angle

Sabya Sachi Chatterjee^{1,2,*}, Pedro Pasquini^{3,†} and J.W.F. Valle^{4‡}

¹ *Institute of Physics, Sachivalaya Marg, Sainik School Post, Bhubaneswar 751005, India*

² *Homi Bhabha National Institute, Training School Complex, Anushakti Nagar, Mumbai 400085, India*

³ *Instituto de Física Gleb Wataghin - UNICAMP, 13083-859, Campinas SP, Brazil*

⁴ *AHEP Group, Institut de Física Corpuscular – C.S.I.C./Universitat de València, Parc Científic de Paterna. C/Catedrático José Beltrán, 2 E-46980 Paterna (València) - SPAIN*

Taking into account the current global information on neutrino oscillation parameters we forecast the capabilities of future long baseline experiments such as DUNE and T2HK in settling the atmospheric octant puzzle. We find that a good measurement of the reactor angle θ_{13} plays a key role in fixing the octant of the atmospheric angle θ_{23} with such future accelerator neutrino studies.

PACS numbers: 12.15.-y, 13.15.+g, 14.60.Pq, 14.60.St

I. INTRODUCTION

The discovery of neutrino oscillations as a result of solar and atmospheric studies constitutes a major milestone in astroparticle physics [1, 2]. Earthbound experiments based at reactors and accelerators have not only provided a confirmation of the oscillation picture but also brought the field into the precision age. Despite the great experimental effort, however, two of the oscillation parameters remain poorly determined, namely the atmospheric mixing angle θ_{23} and the CP violating phase δ_{CP} [3–5]. Underpinning these parameters as well as determining the neutrino mass ordering constitute important challenges in the agenda of upcoming oscillation experiments, needed to establish the three-neutrino paradigm. Concerning the two poorly known neutrino parameters, θ_{23} yields two degenerate solutions [3–5], well known as the octant problem [6]. One of them is known as lower octant (LO): $\theta_{23} < \pi/4$ while the other is termed as higher octant (HO): $\theta_{23} > \pi/4$. The role of θ_{13} and its precise determination has been stressed in early papers [7, 8]. The actual discovery of large θ_{13} that has opened a tremendous opportunity for the long-baseline neutrino oscillation experiments to resolve the octant issue within the standard 3-flavor framework. This may however be just an approximation to the true scenario, which may involve new physics such as non-unitarity [9–12] which may have important effects on the propagation of astrophysical neutrinos [13, 14] non-standard interactions [15] as well as a light sterile neutrino [16].

Recently there have been many papers addressing the octant issue within the standard 3ν scenario [17–23]. However it has also been shown recently that the octant sensitivity may completely change in the presence of the above non-standard features, i.e. non-unitarity [24], non-standard interaction [25] or a light sterile neutrino [26].

In this letter we specifically focus on the reactor angle θ_{13} and on whether an improved precision in its measurement from reactors, combined with results from future long baseline experiments such as DUNE and/or T2HK, could provide a final resolution to the octant puzzle. Taking into account current global neutrino oscillation parameter fits, we forecast the potential of DUNE [27] and T2HK [28] for pinning down the correct octant of θ_{23} . We find that a sufficiently good measurement of the reactor angle θ_{13} directly fixes values of θ_{23} for which the octant of the atmospheric angle can be distinguished.

II. THEORY PRELIMINARIES

Following [29], the appearance and survival oscillation probabilities in the presence of matter can be written approximately as

$$P_{\mu e} \approx 4s_{13}^2 s_{23}^2 \sin^2 \Delta_{31} + 2\alpha \Delta_{31} s_{13} \sin 2\theta_{12} \sin 2\theta_{23} \cos(\Delta_{31} \pm \delta_{CP}) = P_0 + P_I \quad (1)$$

$$P_{\mu\mu} \approx 1 - \sin^2 2\theta_{23} \sin^2 \Delta_{31} - 4s_{13}^2 s_{23}^2 \frac{\sin^2(A-1)\Delta_{31}}{(A-1)^2} \quad (2)$$

where $\alpha = \frac{\Delta m_{21}^2}{\Delta m_{31}^2}$, $\Delta_{31} = \frac{\Delta m_{31}^2 L}{4E}$ and $A = \frac{2EV_{CC}}{\Delta m_{31}^2}$. Here V_{CC} is the charged current potential in earth matter, while L and E are the propagation distance and energy

* sabya@iopb.res.in

† pasquini@ifi.unicamp.br

‡ valle@ific.uv.es, URL: <http://astroparticles.es/>

of the neutrinos, respectively. The \pm sign in front of δ_{CP} corresponds to neutrinos (upper sign) and antineutrinos (lower sign). The term P_0 is the octant sensitive term, whereas the term related to $\sin^2 2\theta_{23}$ generates the octant degeneracy.

An experiment is octant sensitive, if there is always a finite difference between the two probabilities corresponding to the two octants, despite the minimization performed over the different oscillation parameters. Mathematically,

$$\Delta P \equiv P_{\mu e}^{\text{HO}} - P_{\mu e}^{\text{LO}} \neq 0 \quad (3)$$

Note that we assume that one of the two octants is the true octant in order to generate the data, while the other one is the false octant in order to simulate the theoretical model predictions. We will always assume that θ_{13} lies in its true value ($\sin^2 \theta_{13} = 0.0234$) in the true octant. Following Eq. 1, we can write

$$\Delta P = \Delta P_0 + \Delta P_I. \quad (4)$$

Now, by expanding Eq. 1 around $\theta_{23} = \pi/4 \pm \eta$ and $\sin^2 \theta_{13} = (1 + \epsilon) \sin^2 \theta_{13}$ we get,

$$P_0 = (1 \pm 2\eta + \epsilon)P' + O(\epsilon\eta)$$

where $\epsilon = \pm \delta(\sin^2 \theta_{13})$ denotes the error on $\sin^2 \theta_{13}$ and the \pm sign in front of η refers to HO (upper sign) and LO (lower sign) and,

$$P' \equiv P'(\theta_{23} = \pi/4, \theta_{13} = \theta_{13}^{\text{true}}) = 4s_{13}^2 s_{23}^2 \sin^2 \Delta_{31}.$$

leading to

$$\Delta P_0 = (P_0^{\text{HO}} - P_0^{\text{LO}}) = P'(4\eta \pm \epsilon). \quad (5)$$

The double sign in front of ϵ refers to the LO^{true} (upper sign) and HO^{true} (lower sign).

In the same manner, we can also write

$$\Delta P_I = B \left[\sin \theta_{13}^{\text{HO}} \cos(\Delta_{31} \pm \delta_{CP}^{\text{HO}}) - \sin \theta_{13}^{\text{LO}} \cos(\Delta_{31} \pm \delta_{CP}^{\text{LO}}) \right] \quad (6)$$

where, $B = 4 \sin \theta_{12} \cos \theta_{12} (\alpha \Delta) \sin \Delta_{31}$. Notice that, as mentioned above, $\sin \theta_{13}^{\text{HO}}$ and $\sin \theta_{13}^{\text{LO}}$ change shape depending on true versus wrong octant.

For the time being suppose one neglects the error on $\sin^2 \theta_{13}$ by taking $\epsilon \rightarrow 0$. ΔP_0 is positive definite, while ΔP_I can have either sign due to the presence of the unknown δ_{CP} . As a result ΔP may become zero for the unfavorable combinations of octant and δ_{CP} , so that octant

sensitivity can be completely lost. However, it has been noticed in the literature [17, 30] that this type of degeneracy can be lifted by using both neutrino and antineutrino channels and one can achieve good octant sensitivity in the 3-flavor scenario.

In the presence of a nonzero error on $\sin^2 \theta_{13}$, then ΔP_0 is also a positive definite quantity, since the current error on $\sin^2 \theta_{23}$ is bigger than the error on $\sin^2 \theta_{13}$, i.e., we can safely assume $\eta > \epsilon$. In this case it is clear from Eqs. 5 and 6 that the unfavorable contribution coming from $\epsilon \neq 0$ changes the magnitude of ΔP_0 and ΔP_I in such a way that overall value of ΔP decreases further than in the previous case. As a result the octant discrimination sensitivity decreases significantly even in the presence of neutrino and antineutrino channels. The larger the error, the less will be the resulting octant sensitivity. This will be clearly seen in the next section.

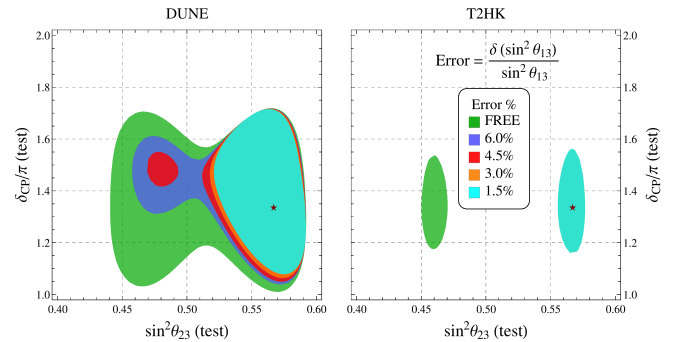


FIG. 1. Precision measurement of θ_{23} and δ_{CP} at 3σ ($\Delta\chi^2 = 9$) confidence. The symbol "star" denotes $\sin^2 \theta_{23}^{\text{TRUE}} = 0.567$ and $\delta_{CP}^{\text{TRUE}} = 1.34\pi$. Left (Right) panels correspond to DUNE (T2HK). Differently shaded (colored) regions correspond to various errors associated with $\sin^2 \theta_{13}$.

III. RESULTS AND DISCUSSION

In this section we present our numerical results and their comprehensive discussion. In our whole analysis we have used a line-averaged constant matter density of 2.95 gm/cm^3 for DUNE and 2.8 gm/cm^3 for T2HK within the PREM [31, 32] profile.

A. Precision measurement

Fig. 1 represents the precision measurement of θ_{23} and δ_{CP} at 3σ confidence for various combinations of the relative error associated with $\sin^2 \theta_{13}$. The symbol "star" in

the body of the plot corresponds to the values $\sin^2 \theta_{23}^{\text{TRUE}} = 0.567$ and $\delta_{\text{CP}}^{\text{TRUE}} = 1.34\pi$ obtained in [3]. The left (right) panel is for DUNE (T2HK). The cyan band corresponds to 1.5%, the orange band corresponds to 3.0%, the red band is for 4.5% and the blue band corresponds to 6.0% error on $\sin^2 \theta_{13}$. In contrast, the green band is generated by the free marginalization over $\sin^2 \theta_{13}$. We have marginalized over Δm_{31}^2 and θ_{12} with prior on $\sin^2 \theta_{12}$. From the left panel, it is clear that DUNE can not exclude the wrong octant up to 5% error, while it can surely exclude the wrong octant at 3σ confidence if $\sin^2 \theta_{13}$ is very tightly constrained, as seen from the cyan shaded region. Thanks to its higher statistics in the disappearance channel, T2HK performs better in this case and can exclude the wrong octant even up to 6% error associated with $\sin^2 \theta_{13}$, i.e., T2HK can measure the atmospheric mixing angle very precisely.

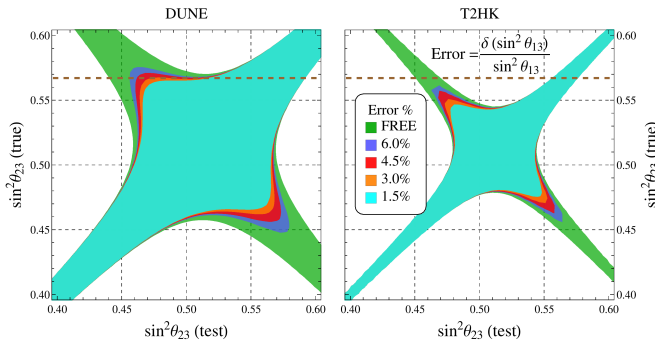


FIG. 2. 3σ precision measurement of θ_{23} . The left (right) panel is for DUNE (T2HK). Differently shaded regions correspond to various errors associated with $\sin^2 \theta_{13}$. The thick dashed line represents the current best fit value from [3].

Now we turn to a very general question, namely, how well can these two experiments measure θ_{23} irrespective of its true value chosen by nature. Fig. 2 addresses this issue. The simulation procedure is exactly the same as for fig. 1, except for the fact that we have marginalized over δ_{CP} both in the data and the theory. As a result this figure represents the most conservative scenario. If we draw a horizontal line for each true value of $\sin^2 \theta_{23}$, it touches the different colored shaded regions associated to different $\sin^2 \theta_{13}$ errors. The horizontal boundary of each touched shaded region corresponding to a particular color represents the 3σ uncertainty on $\sin^2 \theta_{23}$. It can be determined simply by looking at the brown thick dashed line at $\sin^2 \theta_{23}(\text{true}) = 0.567$ and focusing on the cyan band. This procedure extracts all the relevant information coming from fig. 1. It is noticeable that DUNE

measures the LO ($\sin^2 \theta_{23}(\text{true}) < 0.45$) better than the HO. However, the performance of T2HK is substantially higher than that of DUNE in both the octants. An important consequence of the green area in Fig. 2 is the fact that neither DUNE nor T2HK can distinguish the octant without prior knowledge of θ_{13} .

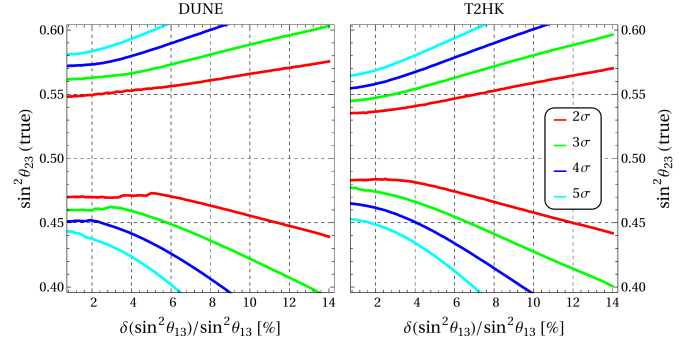


FIG. 3. Octant discrimination potential as a function of the relative error on $\sin^2 \theta_{13}$ for the true value of $\delta_{\text{CP}}^{\text{TRUE}} = 1.34\pi$. The left (right) panel represents the results for DUNE (T2HK). The red, green, blue and cyan curves delimit the θ_{23} “octant-blind” region corresponding to 2, 3, 4 and 5 σ confidence (1 d.o.f.).

B. Octant discrimination

Here we analyse the potential of DUNE and T2HK for excluding the wrong octant provided the data is generated in the true octant. Fig. 3 illustrates the octant sensitivity as a function of the relative error on $\sin^2 \theta_{13}$. The left (right) panel corresponds to the result for DUNE (T2HK). The colored curves indicate the sensitivity for discriminating the false octant from the true one depending on the relative $\sin^2 \theta_{13}$ error. The red, green, blue and cyan correspond to the 2σ , 3σ , 4σ and 5σ confidence level cases, respectively. NH is assumed as the true hierarchy both in data and theory. Concerning theory, we have marginalized over the oscillation parameters θ_{12} , θ_{13} , θ_{23} , δ_{CP} and Δm_{31}^2 within their allowed range, for a given prior on $\sin^2 \theta_{12}$. One sees from the figure that, depending on the $\sin^2 \theta_{13}$ error, the octant sensitivity increases or decreases. For example, from the cyan curve for DUNE or T2HK, one sees that the 1% error corresponds to 5σ sensitivity for $\sin^2 \theta_{23}(\text{true}) < 0.45$ and $\sin^2 \theta_{23}(\text{true}) > 0.58$. As the error increases up to around 6%, the sensitivity is gradually lost. So the measurement of the octant of θ_{23} strongly depends on the relative error of the $\sin^2 \theta_{13}$ determination. The oc-

tant discrimination sensitivity is slightly better for T2HK than DUNE due to its high statistics.

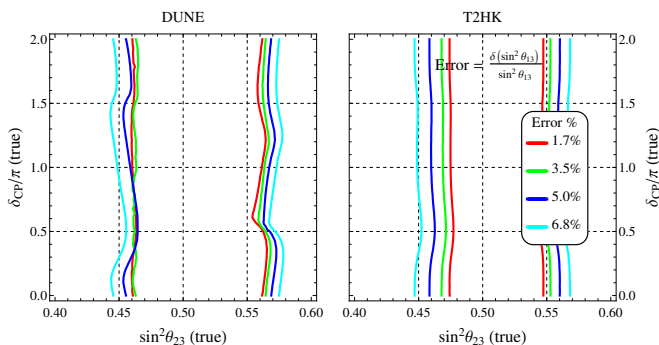


FIG. 4. Octant discrimination potential at 3σ confidence level in the $[\sin^2\theta_{23}, \delta_{CP}]/\pi$ (true) plane. The red, green, blue and cyan curves delimit the “octant-blind” regions corresponding to 1.7%, 3.5%, 5.0% and 6.8% relative errors on $\sin^2\theta_{13}$.

In fig. 3, we generated the data assuming $\delta_{CP}(\text{true}) = 1.34\pi$. So, it is natural to ask what would be the octant sensitivity over the entire $\sin^2\theta_{23}(\text{true})$ and $\delta_{CP}(\text{true})$ plane. Fig. 4 provides a clear answer to this question. The simulation details are exactly the same as for fig. 3. This figure beautifully summarizes the effect of the relative $\sin^2\theta_{13}$ error on the octant sensitivity. We have assumed a 3σ confidence level for the exclusion of the wrong octant and then varied the various error combinations as indicated by the different colors. A band of uncertainty clearly arises, decreasing the 3σ sensitivity range for $\sin^2\theta_{23}(\text{true})$. It is important to notice that our result is almost independent of $\delta_{CP}(\text{true})$. Again, as discussed earlier, T2HK gives slightly better sensitivity than DUNE.

IV. SIMULATION DETAILS

We have assumed standard experimental configurations for the DUNE [27] and T2HK [28] experiments, as given by their corresponding CDR papers. Brief descriptions of the experimental setup of DUNE and T2HK are mentioned in [33]. We have performed a realistic simulation by using the GLoBES package [34, 35]. The best fit values of the oscillation parameters were taken from [3]. They are the following: $\sin^2\theta_{12} = 0.323$, $\sin^2\theta_{13} = 0.0234$, $\sin^2\theta_{23} = 0.567$ (0.573) for NH (IH), $\delta_{CP} = 1.34\pi$, $\Delta m_{21}^2 = 7.5 \times 10^{-5} \text{ eV}^2$, and $\Delta m_{31}^2 = 2.48 \times 10^{-3}$ (-2.38×10^{-3}) eV^2 for NH (IH). Here NH (IH) is short for normal hierarchy (inverted hierarchy). In all of our numerical analysis, we have assumed NH as fixed both in

data and theory. In order to determine the sensitivity towards the measurement of the octant of θ_{23} , we have defined the χ^2 function as,

$$\chi^2 = \chi_{\text{GLoBES}}^2 + \chi_{\text{Priors}}^2 \quad (7)$$

where χ_{GLoBES}^2 is the standard GLoBES Poissonian chi-squared, while χ_{Priors}^2 is given by,

$$\chi_{\text{Priors}}^2 = \left(\frac{s_{12}^{\text{TRUE}} - s_{12}^{\text{TEST}}}{\delta\theta_{12}} \right)^2 + \left(\frac{s_{13}^{\text{TRUE}} - s_{13}^{\text{TEST}}}{\delta\theta_{13}} \right)^2 \quad (8)$$

with $\delta\theta_{ij}$ the $\sin^2\theta_{ij}^{\text{TRUE}}$ error from [3], while $s_{ij}^A = \sin^2\theta_{ij}^A$. Here $A = \text{TRUE}, \text{TEST}$ denote the true and test values of the angles respectively. We have not included either δ_{CP} or θ_{23} priors, as we are focusing on the capability of each experiment to measure them. In order to distinguish the true octant from the false one. We define the chi-squared difference as $\Delta\chi_{\text{oct}}^2 = |\chi_{\text{min}}^2(\theta_{23} \leq \pi/4) - \chi_{\text{min}}^2(\theta_{23} > \pi/4)|$. Here $\chi_{\text{min}}^2(\theta_{23})$ is the χ^2 function minimized over other oscillation parameters. Note that one can assume one of the octants (say, $\theta_{23} \leq \pi/4$) as true and the other one as false, and vice-versa.

Recent reactor experiments have reached a precision at the percent level for the measurement of the reactor angle, fixing its central value around $\sin^2\theta_{13} \sim 0.02$. Current and foreseen precision levels on the reactor angle are given in table I. For the simulation we took the central value of $\sin^2\theta_{13}$ from the global fit [3] and not from the individual reactor experiments. This makes the analysis more robust, as a single experiment cannot give a general picture for the value of $\sin^2\theta_{13}$.

	DC [36]	RENO [37]	Daya-Bay [38]	Global [3]
$s_{13}^2/10^{-2}$	2.85	2.09	2.09	2.34
$\delta\theta_{13}$	16.7%	13.4%	4.9%	8.5%
$\delta\theta_{13}^{\text{Expe}}$	10%	5%	3.6%	<3%

TABLE I. Current and expected values of the reactor mixing angle θ_{13} and its sensitivity for different experiments and current global neutrino oscillation fit.

V. CONCLUSIONS

Based upon the current global information on neutrino oscillation parameters we have performed a quantitative analysis of the potential of upcoming long baseline experiments DUNE and T2HK in resolving the atmospheric octant ambiguity. We have found that a precise measurement of the reactor angle θ_{13} plays a key role in

resolving the octant of the atmospheric angle θ_{23} using such future accelerator neutrino experiments. Our analysis highlights the complementarity of reactor and accelerator-based studies in gaining fundamental information on neutrino properties.

ACKNOWLEDGEMENTS

Work supported by Spanish grants FPA2014-58183-P, Multidark CSD2009-00064, SEV-2014-0398 (MINECO), PROMETEOII/2014/084 (Generalitat Valenciana). P. S. P. acknowledges the support of FAPESP/CAPES grant 2014/05133-1, 2015/16809-9 and 2014/19164-6.

-
- [1] T. Kajita, Rev. Mod. Phys. **88**, 030501 (2016).
 - [2] A. B. McDonald, Rev. Mod. Phys. **88**, 030502 (2016).
 - [3] D. V. Forero, M. Tortola, and J. W. F. Valle, Phys. Rev. **D90**, 093006 (2014), 1405.7540.
 - [4] F. Capozzi, E. Lisi, A. Marrone, D. Montanino, and A. Palazzo, Nucl. Phys. **B908**, 218 (2016), 1601.07777.
 - [5] I. Esteban, M. C. Gonzalez-Garcia, M. Maltoni, I. Martinez-Soler, and T. Schwetz, JHEP **01**, 087 (2017), 1611.01514.
 - [6] G. L. Fogli and E. Lisi, Phys. Rev. **D54**, 3667 (1996), hep-ph/9604415.
 - [7] H. Minakata, H. Sugiyama, O. Yasuda, K. Inoue, and F. Suekane, Phys. Rev. **D68**, 033017 (2003), [Erratum: Phys. Rev.D70,059901(2004)], hep-ph/0211111.
 - [8] M. Maltoni, T. Schwetz, M. A. Tortola, and J. W. F. Valle, New J. Phys. **6**, 122 (2004), hep-ph/0405172.
 - [9] J. W. F. Valle, Phys. Lett. **B199**, 432 (1987).
 - [10] O. G. Miranda and J. W. F. Valle, Nucl. Phys. **B908**, 436 (2016), 1602.00864.
 - [11] O. G. Miranda, M. Tortola, and J. W. F. Valle, Phys. Rev. Lett. **117**, 061804 (2016), 1604.05690.
 - [12] F. J. Escrihuela, D. V. Forero, O. G. Miranda, M. T̃aşr-tola, and J. W. F. Valle (2016), 1612.07377.
 - [13] H. Nunokawa, Y. Z. Qian, A. Rossi, and J. W. F. Valle, Phys. Rev. **D54**, 4356 (1996), hep-ph/9605301.
 - [14] D. Grasso, H. Nunokawa, and J. W. F. Valle, Phys. Rev. Lett. **81**, 2412 (1998), astro-ph/9803002.
 - [15] L. Wolfenstein, Phys. Rev. **D17**, 2369 (1978).
 - [16] T. S. Kosmas, D. K. Papoulias, M. Tortola, and J. W. F. Valle (2017), 1703.00054.
 - [17] S. K. Agarwalla, S. Prakash, and S. U. Sankar, JHEP **07**, 131 (2013), 1301.2574.
 - [18] S. K. Agarwalla, S. Prakash, and S. Uma Sankar, JHEP **03**, 087 (2014), 1304.3251.
 - [19] A. Chatterjee, P. Ghoshal, S. Goswami, and S. K. Raut, JHEP **06**, 010 (2013), 1302.1370.
 - [20] M. Bass et al., Phys. Rev. **D91**, 052015 (2015), 1311.0212.
 - [21] K. Bora, D. Dutta, and P. Ghoshal, Mod. Phys. Lett. **A30**, 1550066 (2015), 1405.7482.
 - [22] C. R. Das, J. Maalampi, J. Pulido, and S. Vihonen, JHEP **02**, 048 (2015), 1411.2829.
 - [23] N. Nath, M. Ghosh, and S. Goswami, Nucl. Phys. **B913**, 381 (2016), 1511.07496.
 - [24] D. Dutta, P. Ghoshal, and S. K. Sehrawat (2016), 1610.07203.
 - [25] S. K. Agarwalla, S. S. Chatterjee, and A. Palazzo, Phys. Lett. **B762**, 64 (2016), 1607.01745.
 - [26] S. K. Agarwalla, S. S. Chatterjee, and A. Palazzo, Phys. Rev. Lett. **118**, 031804 (2017), 1605.04299.
 - [27] R. Acciarri et al. (DUNE) (2015), 1512.06148.
 - [28] K. Abe et al. (Hyper-Kamiokande Proto-Collaboration), PTEP **2015**, 053C02 (2015), 1502.05199.
 - [29] E. K. Akhmedov, R. Johansson, M. Lindner, T. Ohlsson, and T. Schwetz, JHEP **04**, 078 (2004), hep-ph/0402175.
 - [30] P. A. N. Machado, H. Minakata, H. Nunokawa, and R. Zukanovich Funchal, JHEP **05**, 109 (2014), 1307.3248.
 - [31] A. M. Dziewonski and D. L. Anderson, Physics of the Earth and Planetary Interiors **25**, 297 (1981), ISSN 0031-9201, URL<http://www.sciencedirect.com/science/article/pii/0031920181900467>.
 - [32] F. D. Stacey, *Physics of the earth*, vol. 2nd ed. (Wiley, 1977).
 - [33] S. S. Chatterjee, P. Pasquini, and J. W. F. Valle (2017), 1702.03160.
 - [34] P. Huber, M. Lindner, and W. Winter, Comput. Phys. Commun. **167**, 195 (2005), hep-ph/0407333.
 - [35] P. Huber, J. Kopp, M. Lindner, M. Rolinec, and W. Winter, Comput. Phys. Commun. **177**, 432 (2007), hep-ph/0701187.
 - [36] A. Cabrera, *Double chooz (new multi-detector results)*, ep seminar, indico.cern.ch/event/548805/attachments/1336343/2017513/DCIVCERN_REF_Anatael_16Sept.pdf.
 - [37] J. H. Choi et al. (RENO), Phys. Rev. Lett. **116**, 211801 (2016), 1511.05849.
 - [38] F. P. An et al. (Daya Bay) (2016), 1610.04802.